IMPROVEMENTS IN THE TREATMENT OF COMPTON CURRENT AND AIR CONDUCTIVITY IN EMP PROBLEMS

Conrad L. Longmire, et al

Mission Research Corporation

Prepared for:

Defense Nuclear Agency

25 September 1973

UNCLASSIFIED

SECURITY CLASSIFICATION OF THIS PAGE (When Data Entered)

AD 769 914

REPORT DOCUMENTATION PAGE		READ INSTRUCTIONS BEFORE COMPLETING FORM
1. REPORT NUMBER DNA 3192T	2. GOVT ACCESSION NO.	3. RECIPIENT'S CATALOG NUMBER
4. TITLE (and Subtitle) Improvements in the Treatment of Compton Current and Air Conductivity in EMP Problems		5. TYPE OF REPORT & PERIOD COVERED Topical Report 6. PERFORMING ORG. REPORT NUMBER MRC-N-2
7. AUTHOR(s) Conrad L. Longmire H. Jerry Longley		8. CONTRACT OR GRANT NUMBER(s) DASA 01-71-C-0105
9. PERFORMING ORGANIZATION NAME AND ADDRESS Mission Research Corporation 735 State Street, Santa Barbara, California 93101		10. PROGRAM ELEMENT, PROJECT, TASK AREA & WORK UNIT NUMBERS NWED Subtask Code EA 091 Work Unit Code 03
11. CONTROLLING OFFICE NAME AND ADDRESS Director Defense Nuclear Agency Washington, D.C. 20305		12. REPORT DATE 25 September 1973 13. NUMBER OF PAGES 44
14. MONITORING AGENCY NAME & ADDRESS(if different from Controlling Office)		15. SECURITY CLASS. (of this report) UNCLASSIFIED 15a. DECLASSIFICATION/DOWNGRADING SCHEDULE

16. DISTRIBUTION STATEMENT (of this Report)

Approved for public release; distribution unlimited.

17. DISTRIBUTION STATEMENT (of the abstract entered in Block 20, if different from Report)

18. SUPPLEMENTARY NOTES

This report was prepared 22 October 1971.

19. KEY WORDS (Continue on reverse side if necessary and identify by block number)

EMP
Compton Current
Multiple Scattering
Air Conductivity
Ionization
Range of Electrons in Air

20. ABSTRACT (Continue on reverse side if necessary and identify by block number)

This note presents improvements in methods for treating the Compton current and air conductivity in EMP problems, including the effects of multiple scattering of the Compton electrons and formative time lag of the secondary ionization. The problem of equilibration of low energy electrons is also discussed.

DD FORM 1 JAN 73 1473 EDITION OF 1 NOV 65 IS OBSOLETE

UNCLASSIFIED

SECURITY CLASSIFICATION OF THIS PAGE (When Data Entered)

TABLE OF CONTENTS

		PAGE
LIST OF FIGURES		2
SECTION		
1.	INTRODUCTION	3
2.	SLOWING DOWN OF COMPTON RECOIL ELECTRONS	3
3.	MULTIPLE SCATTERING OF COMPTON ELECTRONS	5
4.	MEAN RANGE OF A COLLIMATED BEAM	7
5.	EQUATIONS OF MOTION IN PRESENCE OF ELECTROMAGNETIC FIELDS	11
6.	CHANGE IN η DUE TO FIELDS	14
7.	SPATIAL SPREADING OF A BEAM	15
8.	THE IONIZATION	22
9.	ELECTRON EQUILIBRATION	31
REFERENCES		34

LIST OF FIGURES

FIGURE		PAGE
1.	Transmission of energetic electrons through Aluminum foils.	9
2.	Relation of central momentum $\vec{p}$ to distribution at a given time.	12
3.	Change in moments induced by a force, (a) perpendicular to $\vec{p}$, and (b) antiparallel to $\vec{p}$	14
4.	Graph of $\sigma_i v$ as a function of w for electrons on air atoms.	27
5.	Solid curve, integrand of Eq. (82).	28

1. Introduction

In this note we present improvements in the methods for treating the Compton current and the air conductivity, for use in EMP calculations. Specifically, we shall give:

(a) a method of treating the effect of multiple scattering, as well as slowing down, of the Compton recoil electrons;

(b) a method of treating the time lag between the production of the primary ionization and of the total ionization;

(c) a discussion of the problem of equilibration of the free electrons, from the initial ionization spectrum to the spectrum appropriate to the instantaneous value of E/p .

2. Slowing Down of Compton Recoil Electrons

The energy loss of relativistic electrons in moving through matter is given by Bethe's formula (Ref. 1); per unit track length, it is

$$-\frac{dW}{ds} = \frac{2\pi NZe^4}{mv^2}\,[1] \quad , \tag{1}$$

where

$$[1] = \ell n\left[\frac{(mc^2)^2(\gamma-1)(\gamma^2-1)}{2I^2}\right] - \left(\frac{2}{\gamma}-\frac{1}{\gamma^2}\right)\ell n\ 2 + \frac{1}{\gamma^2} + \frac{1}{8}\left(1-\frac{1}{\gamma}\right)^2 . \tag{2}$$

In these formulae, N is the density of atoms, Z the atomic number, e, m and v the electron charge, rest mass, and velocity, c is the velocity of light, and

$$\gamma = \frac{1}{\sqrt{1-\beta^2}} \quad , \quad \beta = \frac{v}{c} \quad . \tag{3}$$

For air we take the effective atomic number

$$Z = 7.2 \tag{4}$$

and the mean excitation potential I (Ref. 1) to be

$$I = 80.5 \text{ ev} \quad . \tag{5}$$

In solving the equations of motion of a Compton recoil electron, one can take account of the energy loss by imagining that the electron experiences a force directed opposite to $\vec{v}$, of magnitude given by the right-hand side of Eq. (1). This procedure, however, does not yet take into account the multiple scattering of the Compton electrons, which has the following effect. A beam of electrons, directed initially in the x-direction, is greatly broadened in angle by the scattering, so that the electrons spend a lot of their energy moving in directions oblique to the x-direction. Eq. (1) is correct for the energy loss per element of length of the actual trajectory of an individual electron, but its use with ds replaced by dx will overestimate the average distance electrons will travel in the x-direction before stopping.

In the past, we have taken account of the multiple scattering by noting that, experimentally, the mean range of electrons in the Mev region is about 2/3 of the total (or "extreme") range. We have therefore simply multiplied the drag force (right-hand side of Eq. (1)) by a factor 3/2. This procedure, however, gives a wrong distribution of ionization along the path of the Compton electron. The ionization per unit length is proportional

to $-\frac{dW}{dx}$, and is important because it determines the air conductivity. Now at the beginning of a Compton electron track, the multiple scattering has not yet had much effect, and multiplying $\frac{dW}{ds}$ by 3/2 overestimates the ionization per unit length. Similarly, the ionization density is underestimated near the end of the range. In EMP from high altitude bursts, the peak electric field tends to come when the Compton electrons are near the beginning of their range; an overestimate of air conductivity by a factor 3/2 may lead to an underestimate of the peak electric field by the same factor.

Obviously, we need a treatment in which the multiple scattering is allowed to build up along the trajectory.

3. Multiple Scattering of Compton Electrons

We shall use the simple form of multiple scattering theory due to Williams (Ref. 2), which will be adequate for our purpose. According to this theory, the mean squared angle $\overline{\theta^2}$ of an initially collimated beam increases with distance traveled as

$$\frac{d\overline{\theta^2}}{ds} = \frac{8\pi NZ^2e^4}{\gamma^2m^2v^4}\,[2] \tag{6}$$

where

$$[2] = \ln\left(\frac{2}{\theta_{min}}\right) . \tag{7}$$

Here θ_{min} is the minimum angle of scattering, below which the scattered angular distribution falls substantially below that given by the Rutherford formulae. For scattering by neutral atoms, as in our case, θ_{min} is determined by the screening of the nuclear charge by the atomic electrons. For the Fermi-Thomas atomic model, Mott and Massey (Ref. 2) give

$$\theta_{min} = \frac{0.0153\ Z^{1/3}}{\beta\gamma} . \tag{8}$$

Then

$$[2] \quad = \quad \ln\left(\frac{131\sqrt{\gamma^2-1}}{Z^{1/3}}\right) \quad . \tag{9}$$

In Eq's. (6) and (7) we have departed slightly from standard theory, in which $\overline{\theta^2}$ is the mean square angle in only the gaussian part of the angular distribution. Then the argument of the logarithm in Eq. (7) becomes (θ_1/θ_{min}), where θ_1 depends on s, and is the angle below which the scattering is multiple. However, we are using $\overline{\theta^2}$ as the mean square angle of the entire angular distribution, in which case the argument $(2/\theta_{min})$ is correct (Ref. 3).

Eq. (6) is strictly correct only when $\overline{\theta^2}$ is small, where successive scattering angles add linearly. Consider, however, the obliquity factor

$$\eta \quad \equiv \quad \frac{1}{\cos\theta} \quad . \tag{10}$$

This factor relates the differential track length ds to the distance dx in the direction of initial collimation,

$$ds \quad = \quad \eta\, dx \quad . \tag{11}$$

For small θ,

$$\eta \quad \approx \quad 1 + \frac{\theta^2}{2} \quad , \tag{12}$$

so that Eq. (6) becomes

$$\frac{d\overline{\eta}}{ds} \quad = \quad \frac{4\pi N Z^2 e^4}{\gamma^2 m^2 v^4}\,[2] \quad . \tag{13}$$

For large mean angles of scattering, this equation has the virtue that near

the end of the range, where $\bar{\eta}$ will become infinite, the mean $\cos\theta$ will become zero, according to Eq. (10); thus all correlation to the initial direction is lost. This is a desirable result, whereas having $\overline{\theta^2}$ become infinite (as results from Eq. (6)) is not. We shall therefore use Eq. (13) instead of Eq. (6), and note that $\bar{\eta}$ starts at unity for an initially collimated beam.

4. Mean Range of a Collimated Beam

Suppose that we have a monoenergetic beam, collimated in the x direction, entering a slab of material. Then the equations for the change in kinetic enegy W and obliquity factor η (we drop the bar on $\bar{\eta}$) are

$$\frac{d\eta}{dx} = f(W)\,\eta \quad , \tag{14}$$

$$\frac{dW}{dx} = -g(W)\,\eta \quad , \tag{15}$$

where

$$f(W) = \frac{4\pi NZ^2e^4\gamma^2}{(mc^2)^2(\gamma^2-1)^2}\,[2] \quad , \tag{16}$$

$$g(W) = \frac{2\pi NZe^4\gamma^2}{mc^2(\gamma^2-1)}\,[1] \quad . \tag{17}$$

Dividing Eq. (14) by Eq. (15) and using

$$W = (\gamma-1)\,mc^2 \quad , \tag{18}$$

we find

$$d\eta = -\frac{2Z}{\gamma^2-1}\,\frac{[2]}{[1]}\,d\gamma \tag{19}$$

Now, it turns out that the ratio

$$\Gamma \equiv \frac{[2]}{[1]} \tag{20}$$

is very nearly independent of energy W or γ. For example, for air (see Eq's (4) and (5)) we find:

W	γ	Γ
51 Kev	1.1	0.262
255 Kev	1.5	0.266
511 Kev	2.0	0.269
1.02 Mev	3.0	0.270
1.53 Mev	4.0	0.271

Clearly, for our purposes, Γ can be taken as constant. We shall use the values,

$$\left.\begin{aligned} \Gamma &= 0.269 \text{ in air} \quad , \\ \Gamma &= 0.276 \text{ in aluminum} \quad . \\ &\quad (I = 150\text{ev for aluminum}) \end{aligned}\right\} \tag{21}$$

With the approximation of constant Γ, Eq. (19) can be integrated directly, with the result,

$$\eta = 1 + 2\Gamma \ln\left[\frac{(\gamma_0-1)(\gamma+1)}{(\gamma_0+1)(\gamma-1)}\right] \quad . \tag{22}$$

Here γ_0 is the value of γ for the initial energy of the electrons in the beam.

On using Eq. (22) in Eq. (15), one can integrate (numerically) to find the mean range including the effect of multiple scattering. We have done this for aluminum, and also have calculated the extreme range, which is obtained by omitting the factor η in Eq. (15). In Fig. (1) we compare our results with data of Marshall and Ward (Ref. 4) on the transmission of electrons through foils of aluminum. In the figure, the solid curves

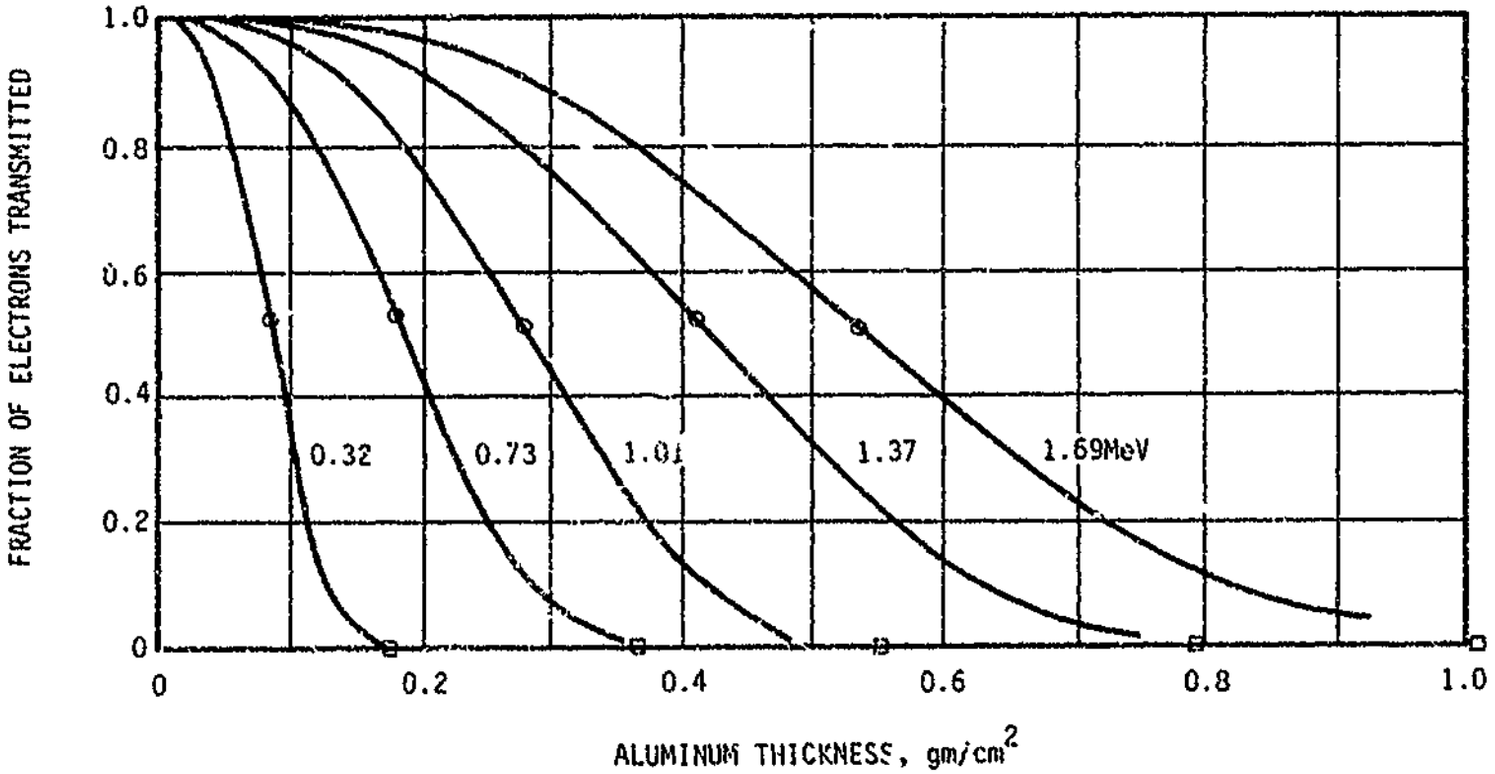

Figure 1. Transmission of energetic electrons through Aluminum foils. Solid curves, data of Marshall and Ward. Squares, calculated extreme ranges. Circles, calculated mean ranges.

represent Marshall's and Ward's measurements of the fraction of initial electrons transmitted as a function of thickness of the foil, for various starting electron energies from 0.32 to 1.69 Mev. The squares placed on the abscissa are at the extreme ranges computed by us using the Bethe formula directly; the agreement with the end points of the experimental curves is very good. The circles placed on the experimental curves are at the mean ranges computed by us using Eq's (15) and (22). Our theory would be well verified if the circles also represented the mean abscissae of the experimental curves. We consider the agreement between theory and data to be quite adequate for our purposes.

In Sec. 5 we shall combine this treatment of energy loss and multiple scattering with equations of motion for the electrons in the presence of fields. Before turning to that task, we record in Table I the mean and extreme ranges of electrons in air, as computed from the above theory, since these results are of general interest.

Table I

Ranges of Electrons in Air

Kinetic Energy W, Mev	Mean Range R_m, gm/cm^2	Fit to Mean Range	Extreme Range R_e, gm/cm^2
0.05	0.0030	0.0029	0.0045
0.1	0.0096	0.0100	0.0157
0.2	0.030	0.032	0.050
0.5	0.120	0.125	0.198
1.0	0.304	0.308	0.489
2.0	0.711	0.695	1.085
5.0	2.01	1.89	2.78

It may be useful to note that the mean range can be fitted, over the energy range in the table, by the simple formula

$$R_m(\text{gm/cm}^2) = \frac{0.40\ W^2}{0.30+W} \qquad (23)$$

Table I also contains values computed from this formula.

5. Equations of Motion in Presence of Electromagnetic Fields

We shall now write equations of motion for the Compton recoil electrons, in the presence of electric and magnetic fields $\vec{E}$ and $\vec{B}$, and taking account of energy loss and multiple scattering.

If no account were taken of multiple scattering, but energy loss were included, the equations of motion would be

$$\frac{d\vec{p}}{dt} = -|e|\left(\vec{E} + \frac{\vec{v}}{c} \times \vec{B}\right) - g(W)\frac{\vec{p}}{|p|} \quad , \tag{24}$$

$$\frac{d\vec{r}}{dt} = \vec{v} \quad . \tag{25}$$

Here $g(W)$ is the energy loss function defined by Eq. (17), $\vec{r}$ is the position of the electron, t is the time, and $\vec{p}$ is the electron momentum. The relations between $\vec{p}$ and $\vec{v}$ and W are

$$\frac{\vec{v}}{c} = \frac{\vec{p}}{\sqrt{p^2+m^2c^2}} \quad , \qquad W = \sqrt{p^2c^2+m^2c^4} - mc^2 \quad . \tag{26}$$

Integration of Eq's (24) and (25) would lead to precise trajectories, with the electrons being deflected by the fields and slowed by the energy loss term.

Now consider the multiple scattering. Since we have already accounted for energy loss, it is necessary only to account for the fluctuations in the angles of $\vec{p}$, without additional changes in the magnitude of $\vec{p}$. The result of the many small and random changes $\delta\vec{p}$ (with $\delta\vec{p} \perp \vec{p}$) will be to make a probability distribution in $\vec{p}$. The value of $\vec{p}$ calculated from Eq. (24), without scattering, will be the central $\vec{p}$ of this distribution, and the distribution will tend to be over momenta having the same magnitude, as in Fig. (2a), although the electric field $\vec{E}$ can lead to situations as illustrated in Fig. (2b).

(a) (b)

Figure 2. Relation of central momentum $\vec{p}$ to distribution at a given time.

Therefore, we retain Eq's (24) and (26) for the central momentum. The average velocity of the distribution, however, is less than the value appropriate to $\vec{p}$, by the mean obliquity factor η. Therefore, we replace Eq. (25) by

$$\frac{d\vec{r}}{dt} = \frac{\vec{v}}{\eta} \tag{27}$$

where $\vec{v}$ is calculated from Eq. (26) from the central momentum. The equation for η is taken over from Eq. (14),

$$\frac{d\eta}{dt} = v\, f(W) \quad . \tag{28}$$

Repeating, we take the equations of motion to be Eq's (24), (26), (27) and (28). The Compton current contributed by an electron (really a distribution of electrons) is taken as

$$\vec{j} = -\frac{|e|}{c}\frac{d\vec{r}}{dt} = -\frac{|e|}{c}\frac{\vec{v}}{\eta} \quad . \tag{29}$$

The time rate of production of ion pairs by the electron is taken as

$$\frac{dI}{dt} = v\, g(W)/w_i \quad . \tag{30}$$

where w_i is the energy expended per ion pair.

Notice that the equations of motion chosen above reduce to Eq's (14) and (15) in the absence of fields. For in that case the central momentum will remain in the x direction if initially pointed in it, and from Eq. (27) we find,

$$dx = \frac{v}{\eta}\, dt \quad . \tag{31}$$

Thus Eq. (28) immediately reduces to Eq. (14). Further, since

$$dW = \vec{v} \cdot d\vec{p} \quad , \tag{32}$$

Eq. (24) reduces to Eq. (15).

In some cases, it is convenient to use the retarded time (r = distance from burst point),

$$t_r = t - \frac{r}{c} \quad , \tag{33}$$

rather than t in the equations of motion. The change to retarded time is accomplished through the relation

$$dt_r = dt - \frac{dr}{\eta c} \quad . \tag{34}$$

$$= \left(1 - \frac{v_r}{\eta c}\right) dt \quad . \tag{34}$$

Here v_r is the radial component of the velocity computed from Eq. (26).

6. Change in η Due to Fields

Eq. (28) shows how η increases with time due to the multiple scattering. We shall see now that additional changes in η occur if the electric field has a component $E_{\parallel}$ parallel to the central $\vec{p}$.

First, it is clear that the magnetic field, and the component $E_{\perp}$ of the electric field perpendicular to $\vec{p}$ cause no direct change in η. In Figure 3 let the solid vectors represent central and extreme momenta

(a) (b)

Figure (3) Change in momenta induced by a force, (a) perpendicular to $\vec{p}$, and (b) antiparallel to $\vec{p}$.

initially, and the dashed vectors represent the same after action of a perpendicular force in (a) and an antiparallel force in (b). In case (a) the entire bundle of momenta is deflected, but the angular spread is not changed in first order. But in case (b) the angular spread obviously increases. If the force were parallel to $\vec{p}$, the angular spread would decrease.

For a given momentum in the bundle of momenta, let $p_{\parallel}$ be the component parallel to the central momentum, and $p_{\perp}$ the perpendicular component. The angle θ this momentum makes with the central momentum is given by

$$\tan\theta = p_{\perp}/p_{\parallel} \quad . \tag{35}$$

From Eq. (10) one can find, by trigonometry,

$$\tan\theta = \sqrt{\eta^2-1} \quad . \tag{36}$$

Therefore,

$$\eta = \sqrt{\left(\frac{p_\perp}{p_\parallel}\right)^2 + 1} \quad . \tag{37}$$

Let there be an electric field $E_\parallel$ parallel to the central $\vec{p}$. Then the equations of motion are

$$\begin{aligned} \frac{dp_\parallel}{dt} &= -|e|\, E_\parallel \quad , \\ \frac{dp_\perp}{dt} &= 0 \quad . \end{aligned} \tag{38}$$

Then, differentiating Eq. (37) with respect to time yields

$$\begin{aligned} \frac{d\eta}{dt} &= -\frac{p_\perp{}^2/p_\parallel^3}{\eta}\,\frac{dp_\parallel}{dt} = |e|\,\frac{\eta^2-1}{\eta}\,\frac{E_\parallel}{p_\parallel} \\ &= |e|\,(\eta^2-1)\frac{\vec{E}\cdot\vec{p}}{p^2} \quad . \end{aligned} \tag{39}$$

where, in the last line, $\vec{p}$ is the central $\vec{p}$.

Therefore, to include the effects of both multiple scattering and $E_\parallel$, Eq. (28) must be replaced by

$$\frac{d\eta}{dt} = v\, f(W) + |e|\,(\eta^2-1)\frac{\vec{E}\cdot\vec{p}}{p^2} \quad . \tag{40}$$

7. Spatial Spreading of a Beam

As a result of the angular spread in velocity induced by multiple scattering, an initially collimated beam will also spread in space, around

the central point determined from the equations of motion derived above. We shall discuss this spreading in an approximate way, valid when the angular spread is small, and in the absence of fields. We shall use the Boltzmann equation, which determines the evolution of the distribution function $\psi(\vec{r},\vec{v})$ in phase space,

$$\frac{\partial\psi}{\partial t} + \vec{v} \cdot \nabla\psi \quad = \quad \text{collision terms} \tag{41}$$

The collision terms have two effects. First, the magnitude of the velocity v of a given particle is gradually decreased with time. The average decrease in v corresponds to the energy loss given by Eq. (1). There are also fluctuations in the energy loss, which give rise to a spread in the magnitude of v at a given time; this in turn gives rise to a spread in position of the particle at a given time. However, this spread in position is less important than that induced by fluctuations in the direction of $\vec{v}$, which we discuss below. Therefore we shall assume that the magnitude v decreases smoothly with time, and ignore the spread in v. However, we shall give below an estimate of the effect of the spread in v.

The other effect of the collision terms is to cause fluctuations in the direction of $\vec{v}$. Because the scattering angle per collision is predominantly very small, the spreading in direction of $\vec{v}$ can be treated in the diffusion approximation, with

$$\text{collision terms} \quad \approx \quad \alpha \nabla_\theta^2 \psi \quad . \tag{42}$$

Here ∇_θ^2 is the angular part of the Laplacian operator in velocity (rather than coordinate) space, and α is (one fourth of) the mean square scattering angle per unit time. This quantity has already been used in Sec.'s (3) and (4) above, and in fact we have (as will be verified below)

$$\alpha(\text{sec}^{-1}) \quad = \quad \frac{v}{2} f(W) \quad . \tag{43}$$

We now choose a Cartesian coordinate system in which the x-axis is parallel to the initial velocity of the collimated beam. We introduce two-dimensional vectors for the two othogonal directions, defining

$$\vec{r} \equiv (y,z) \quad , \quad \nabla \equiv \left(\frac{\partial}{\partial y}, \frac{\partial}{\partial z}\right) \quad . \tag{44}$$

For the velocity, θ will denote the angle between $\vec{v}$ and the x-axis. When θ is small, it can be thought of as being composed of a deflection θ_y in the y-direction and a deflection θ_z in the z-direction. (Two numbers are required to specify the direction of the velocity.) Thus we may regard θ as a vector,

$$\vec{\theta} = (\theta_y, \theta_z) \quad , \quad \nabla_\theta^2 = \frac{\partial^2}{\partial \theta_y^2} + \frac{\partial^2}{\partial \theta_z^2} \quad . \tag{45}$$

The velocity then has components, to first order

$$\left.\begin{aligned} v_x &= v\left(1 - \frac{\theta^2}{2}\right) \qquad \text{parallel to x-axis} \\ \vec{v} &= v\,\vec{\theta} \qquad\qquad\quad \text{parallel to yz plane} \end{aligned}\right\} \tag{46}$$

(Note that $\vec{v}$ here is two dimensional, and will be until further notice.)

In this notation, the Boltzmann equation becomes

$$\frac{\partial}{\partial t}\psi(x,\vec{r},\vec{\theta},t) + v\left(1 - \frac{\theta^2}{2}\right)\frac{\partial \psi}{\partial x} + v\vec{\theta}\cdot\nabla\psi = \alpha\,\nabla_\theta^2\,\psi \tag{47}$$

In this equation, v is understood to decrease smoothly with time; α also changes with time, from Eq. (43). We shall normalize the initial ψ to unity,

$$\int \psi(x,\vec{r},\vec{\theta},0)\,d\tau = 1 \quad , \quad d\tau \equiv dx\,dy\,dz\,d\theta_y\,d\theta_z \quad . \tag{48}$$

By integrating Eq. (47) over phase space, it follows that ψ is so normalized at all times,

$$\frac{\partial}{\partial t}\int \psi(x,\vec{r},\vec{\theta},t)d\tau \quad = \quad 0 \quad . \tag{49}$$

We have assumed here that ψ and its derivatives vanish for large values of its arguments.

The average value of x at time t is

$$\bar{x}(t) \quad = \quad \int x\, \psi(t)d\tau \quad , \tag{50}$$

Multiplying Eq. (47) by x and integrating over phase space, we find

$$\frac{d}{dt}\bar{x} \quad = \quad v\int\left(1 - \frac{\theta^2}{2}\right)\psi\, d\tau \quad = \quad v\left(1 - \frac{\overline{\theta^2}}{2}\right) \quad . \tag{51}$$

Similarly, multiplying Eq. (47) by θ^2 and integrating, we find

$$\frac{d}{dt}\overline{\theta^2} \quad = \quad 4\alpha \qquad (\nabla_\theta{}^2\theta^2 \; = \; 4) \quad . \tag{52}$$

Comparing this result with Eq. (28), we see that Eq. (43) is verified.

Let us now calculate the spread in x. Note that

$$\overline{\Delta x^2} \quad \equiv \quad \overline{(x-\bar{x})^2} \quad = \quad \overline{x^2} - \bar{x}^2 \quad . \tag{53}$$

Thus we need to calculate $\overline{x^2}$. Multiplying Eq. (47) by x^2 and integrating, we find

$$\frac{d}{dt}\overline{x^2} \quad = \quad 2v\,\overline{x\left(1 - \frac{\theta^2}{2}\right)} \quad = \quad 2v\left[\bar{x} - \frac{\overline{x\theta^2}}{2}\right] \quad . \tag{54}$$

Thus we need to find $\overline{x\theta^2}$. In the usual way, we find

$$\begin{aligned}\frac{d}{dt}\overline{x\theta^2} \quad &= \quad v\,\overline{\theta^2\left(1 - \frac{\theta^2}{2}\right)} + 4\alpha\bar{x} \\ &= \quad v\left[\overline{\theta^2} - \frac{\overline{\theta^4}}{2}\right] + 4\alpha\bar{x} \quad .\end{aligned} \tag{55}$$

Now we need $\overline{\theta^4}$, which is determined by

$$\frac{d}{dt}\overline{\theta^4} = 16\,\alpha\,\overline{\theta^2} \quad . \tag{56}$$

These relations may be condensed a bit by noting that

$$\frac{d}{dt}\overline{\Delta x^2} = \frac{d}{dt}\overline{x^2} - 2\bar{x}\frac{d\bar{x}}{dt} = v[\bar{x}\,\overline{\theta^2} - \overline{x\theta^2}] \quad . \tag{57}$$

The quantities on the right here have to be found from Eq's (51), (52), (55), and (56). All of these equations have to be integrated taking into account the dependence of v and α on t . It is instructive, however, to obtain an approximate answer by regarding v and α as constants. One then finds

$$\overline{\theta^2} = 4\alpha t \quad , \tag{58}$$

$$\bar{x} = vt(1-\alpha t) \quad , \tag{59}$$

$$\overline{\theta^4} = 32(\alpha t)^2 \quad , \tag{60}$$

$$\overline{x\theta^2} = vt\left|4\alpha t - \frac{20}{3}(\alpha t)^2\right| \quad , \tag{61}$$

$$\overline{\Delta x^2} = \frac{2}{3}(vt)^2(\alpha t)^2 = \frac{2}{3}(vt - \bar{x})^2 \quad . \tag{62}$$

From Eq. (62) we see that the spread in x is comparable with the amount by which $\bar{x}$ falls behind vt , the position the particle would have if there were no scattering. This result is in substantial agreement with the curves of Fig. (1).

We are also interested in the lateral spread of the beam. To this end, one caiculates from Eq. (47),

$$\frac{d}{dt}\overline{r^2} = 2v\,\overline{\vec{\theta}\cdot\vec{r}} \quad , \tag{63}$$

$$\frac{d}{dt}\overline{\vec{\theta}\cdot\vec{r}} = v\,\overline{\theta^2} \quad . \tag{64}$$

In the approximation that v and α are constants, these equations integrate to

$$\overline{\vec{\theta}\cdot\vec{r}} = 2(vt)(\alpha t) \quad , \tag{65}$$

$$\overline{r^2} = 2(vt)^2(\alpha t) \quad , \tag{66}$$

$$\overline{y^2} = \overline{z^2} = \frac{1}{2}\overline{r^2} = (vt)^2(\alpha t) \quad . \tag{67}$$

One sees that the lateral spread builds up more rapidly than the spread in the x-direction.

If we had considered the fluctuations in the magnitude of v, there would have been an additional term in $\overline{\Delta x^2}$

$$\delta(\overline{\Delta x^2}) \approx (vt)^2\ (\beta t) \quad ; \tag{68}$$

where β is the mean square (fractional) fluctuation in v per unit time,

$$\frac{d}{dt}\overline{\delta v^2} = 2\,v^2\,\beta t \tag{69}$$

The rate β is smaller than the rate α by the ratio

$$\frac{\beta}{\alpha} \approx \frac{1}{\gamma^2 Z[2]} \quad . \tag{70}$$

Here $[2]$ is given by Eq. (9). The factor γ^2 enters because, when $v \approx c$, substantial changes in energy lead to only small changes in the velocity. The factor Z occurs because energy loss is due to collisions with electrons, while angular scattering is due mainly to collisions with the nuclei. The factor $[2]$ occurs because the average of θ^2 involves a logorithmic integral in Rutherford scattering while the average of $(\delta v)^2 \sim \theta^4$ does not. In air, β is only a few percent of α. Thus

while the contribution to $\overline{\Delta x^2}$ in Eq. (68) rises as a lower power of time than that from Eq. (62), by the time at which the multipie scattering becomes important, the terms in Eq. (62) are dominant.

As a numerical example, consider an electron beam that starts with 1 Mev ($\gamma_0 \approx 3$) , and let us examine the distribution when the energy has fallen to 0.5 Mev ($\gamma \approx 2$) . According to Eq. (22), we will then have $\eta \approx 1.79$, for air. Then from Eq. (10), $\overline{\theta^2} \approx 1$, so that from Eq. (58), $\alpha t \approx 1/4$. From Eq's (59), (62) and (67) we then find

$$\bar{x} \approx \frac{3}{4} vt \quad ,$$

$$\sqrt{\overline{\Delta x^2}} \approx \frac{1}{5} vt \quad , \quad \sqrt{\overline{\Delta y^2}} = \sqrt{\overline{\Delta z^2}} \approx \frac{1}{2} vt \quad .$$

Thus the lateral spread in position of the particle is about 2/3 of the mean distance the particles have traveled at this time.

We see that the spread in position is appreciable, and could have noticeable effects if included in EMP calculations. We do not propose that the spatial spread be included in all EMP calculations, but believe that the method of Sections (5) and (6), using the average position, is adequate for most purposes.

However, occasionally we may want to make a calculation including the full effects of multiple scattering. We believe that the best way to do this is to add random velocity changes $\delta\vec{v}$ as the equations of motion of the Compton electrons are being solved. Then, of course, the factors η should be removed from the equations of motion. The drag force, which gives the mean energy loss, should probably be left in the equations of motion. Then to first order, the fluctuations $\delta\vec{v}$ should be such as to leave the magnitude v unaltered; however, fluctuations in $\delta\vec{v}$ could also be included, provided the average $\overline{\delta v}$ is kept equal to zero.

It is not necessary to make the probability distribution of $\vec{\delta v}$ match the Rutherford scattering law. As long as $|\vec{\delta v}| << v$, it is necessary only to make $\overline{\delta\theta^2}$ and $\overline{\delta v^2}$ have the correct mean rates of increase (see, e.g., Eq's (52) and 43)).

8. The Ionization

We now turn to another effect of the Compton electrons, namely the ionization they produce in the air. This is important because it determines the electrical conductivity of the air.

It is well known that fast electrons, in moving through air, produce one ion pair for (about) each 34 ev of energy lost by the fast electrons. Not all of this ionization, however, is produced directly by the fast electron. Rather, some of the electrons dislodged by the fast electron have enough energy to produce further ionization. Ionization produced directly by the fast electron is called the primary ionization, and further ionization is called the secondary ionization. The secondary ionization builds up gradually in time after production of the primary ionization. The time lag in formation of the secondary ionization is important for EMP at high altitudes.

The cross section for ionization of atoms by fast electrons was also computed by Bethe (Reference 5). The cross section has also been measured for some gases, including N_2 and O_2, by Schram and collaborators (Reference 6). Using the experimental data to evaluate uncertain parameters in Bethe's formula, we have deduced the following formula for the ionization cross section per atom of air:

$$\sigma_i \text{ (air atom)} = \frac{2\pi a_0^2 (e^2/a_0)}{mv^2} M_I^2 [3] \quad , \tag{71}$$

where a_0 is the Bohr radius and

$$[3] = \ell n \frac{mv^2}{2V} + 2\ell n\gamma - 1 + \frac{1}{\gamma^2} \quad , \tag{72}$$

with

$$M_I^2 = 4.05, \quad V = 16 \text{ ev for air.} \tag{73}$$

The number of ion pairs I produced per unit length by the fast electron is

$$\frac{dI}{ds} = N\sigma_i, \tag{74}$$

where N is the density of air atoms, as before. Comparing this equation with Eq. (1), we can compute the energy lost per ion pair of primary ionization,

$$-\frac{dW}{dI} = \frac{e^2}{a_0}\,\frac{Z}{M_I^2}\,\frac{[1]}{[3]}\,. \tag{75}$$

We have evaluated this result for several electron energies, and obtain the numbers in Table 2.

Table 2

γ =	1.1	1.5	2.0	3.0	4.0
$\frac{\text{ev}}{\text{ion pair}}$ =	80.0	84.5	85.4	86.4	86.9

It is seen that $\frac{dW}{dI}$ does not change much over the range of interest; we shall use the constant value 86 ev/ion pair.

Thus we find that the total ionization is a factor 86/34 = 2.52 larger than the primary ionization, i.e., each secondary electron must produce, directly and indirectly, 1.52 additional electrons, on the average. We need to find out how this residual ionization builds up in time.

First, it may occur to the reader that the Auger effect, following ejection of a K-shell electron, should result in a practically instantaneous increase of a few per cent in the number of free electrons. However, multiple ionization, including Auger effect, was already included in the

experiments of Schram et al, since they measured electric current rather than counting ionization events.

To estimate the time to form the residual ionization, we must know something about the spectrum of energy w of the secondary electrons (i.e., primary ionization). There appears to be no experimental data on this spectrum. Theoretically, it is expected to be approximately of the form dw/w^2, as in Rutherford scattering. Atomic binding will provide a cutoff of the divergence at $w=0$. We shall therefore assume that the number dn of secondary electrons having energy in dw is:

$$dn = \frac{A\, dw}{w_0^2 + w^2} \quad . \tag{76}$$

To normalize this form to unity, we integrate from $w=0$ to $w=W/2$, where W is the energy of the primary electron; we define the secondary electron to be that one of the two outgoing electrons which has the smaller energy:

$$1 = \int_0^{W/2} dn = \frac{A}{w_0} \arctan\left(\frac{W}{2w_0}\right) = \frac{\pi}{2}\,\frac{A}{w_0} \quad . \tag{77}$$

In the last form here, we have taken advantage of the fact that $W/2w_0$ is (usually) a very large number.

From Equations (76) and (77), we can calculate the mean energy of the secondary electrons:

$$\bar{w} = \frac{2w_0}{\pi} \int_0^{W/2} \frac{w\,dw}{w^2_0 + w^2} = \frac{w_0}{\pi} \ln\left(1 + \frac{W^2}{4w_0^2}\right) . \tag{78}$$

This result can be used to determine an approximate value for the constant w_0. We have seen above that for each free electron produced, the primary electron loses, on the average, 86 ev. Of this, we estimate 20 ev is expended for the ionization potential and another 10 ev left in excitation of atoms (or molecules). Thus the mean kinetic energy $\bar{w}$ of the secondary electrons should be about 56 ev. Taking $W = 10^6$ ev in Equation (78), one then finds:

$$w_0 \simeq 8.0 \text{ ev.} \tag{79}$$

This result seems reasonable, and is probably not in error by more than 20%.

Most of the secondary electrons in the distribution (76) have low energy. The fraction $n(w_1)$ of electrons having $w < w_1$ is

$$n(w_1) = \frac{2}{\pi}\arctan\left(\frac{w_1}{w_0}\right), \tag{80}$$

which leads to numbers in Table 3

Table 3

(w_1/w_0) =	1	2	3	4	∞
$n(w_1)$ =	0.50	0.71	0.80	0.85	1

On the other hand, the energy in the secondary electrons is spread over a large range. The fraction $F(w_1)$ of the secondary energy contained by electrons of energy $w < w_1$ is

$$F(w_1) = \frac{\ell n\left(1 + \frac{w_1^2}{w_0^2}\right)}{\ell n\left(1 + \frac{W^2}{4w_0^2}\right)} . \tag{81}$$

With $W = 10^6$ ev and $W_0 = 8.0$ ev, this formula yields the numbers in Table 4.

Table 4

$\frac{w_1}{w_0}$ =	1	10	10^2	10^3	10^4	10^5
$F(w)$ =	0.03	0.21	0.42	0.62	0.83	1.00

We see that equal amounts of secondary energy are contained in each decade. Since the amount of secondary ionization is approximately proportional to the kinetic energy available, the secondary ionization also will come equally from each decade.

Figure (4) is a graph of $\sigma_i v$ for electrons on air atoms. In plotting this graph we have used experimental data directly, rather than Eq. (71), which is not very accurate for energies less than about 10^3 ev.

The initial rate R_0 of production of ionization by secondary electrons, per secondary electron, is

$$R_0 = N \int \sigma_i v \, dn = N \int \frac{2}{\pi} \frac{\sigma_i v w_0 w}{w_0^2 + w^2} \, d(\ell n \, w) \, . \tag{82}$$

A numerical evaluation of this integral leads to the result

$$R_0 = (1.04 \times 10^{-8} \text{ cm}^3/\text{sec.}) \, N \, . \tag{83}$$

This rate of production of ionization will not be maintained very long. Fig. (5) is a graph of the integrand in Eq. (82), i.e. the factors multiplying $d(\ell n \, w)$. One sees that most of the integral (5/6 of it, in fact) comes from electrons in the energy decades below about 250 ev. According to Eq. (81), or the table following it, only about 30% of the total secondary ionization arises from secondary electrons in this energy range. The initial ionization rate therefore cannot persist for a time longer than

$$T \approx \frac{0.3 \times 1.52}{\frac{5}{6} \, 1.04 \times 10^{-8} N} = \frac{5.3 \times 10^7}{N} \text{ sec.} \tag{84}$$

In fact, the rate should have fallen by a factor 4 or 5 by this time, since the secondaries with energy less than 250 ev will have been exhausted.

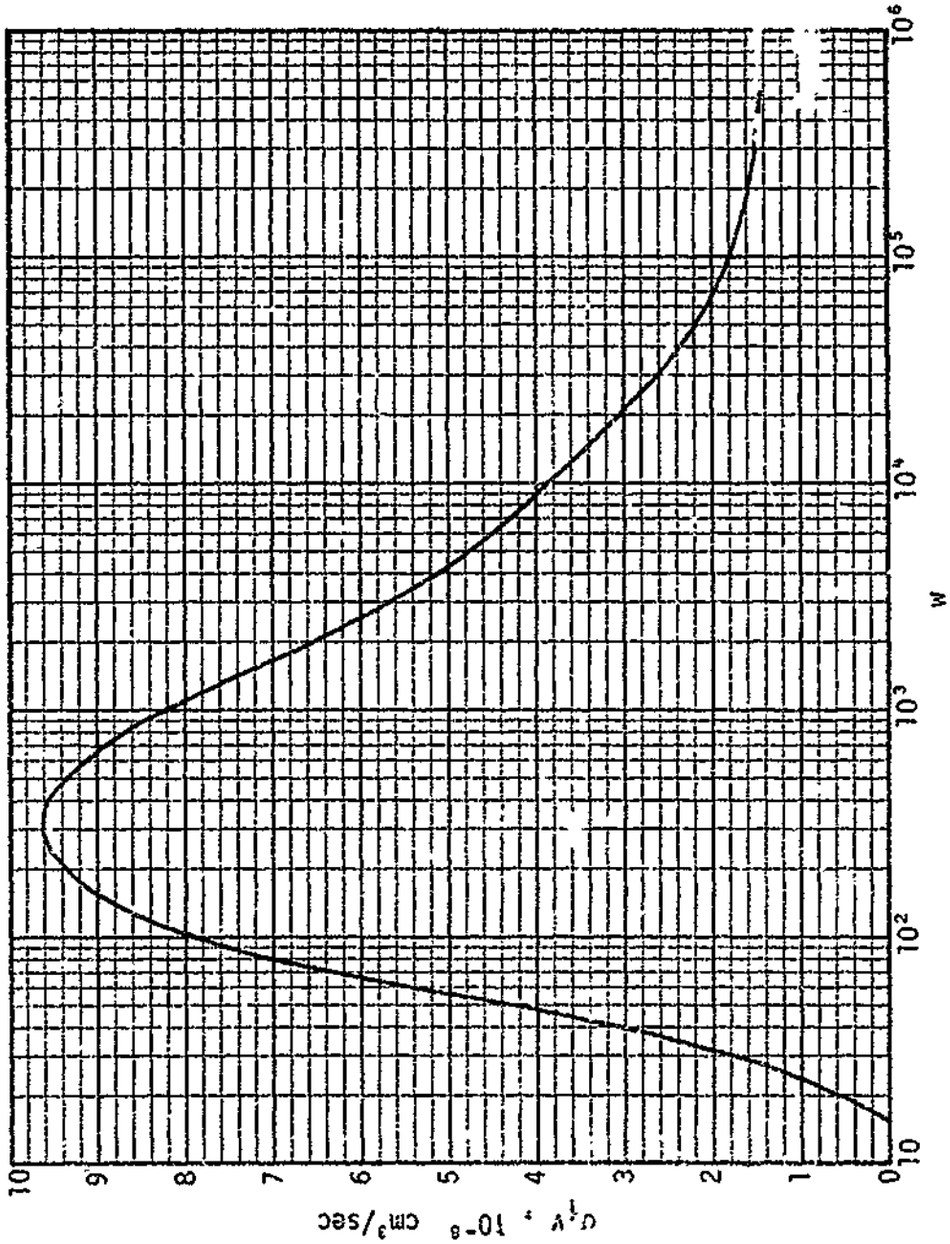

Figure 4. Graph of $\sigma_i v$ as a function of w for electrons on air atoms.

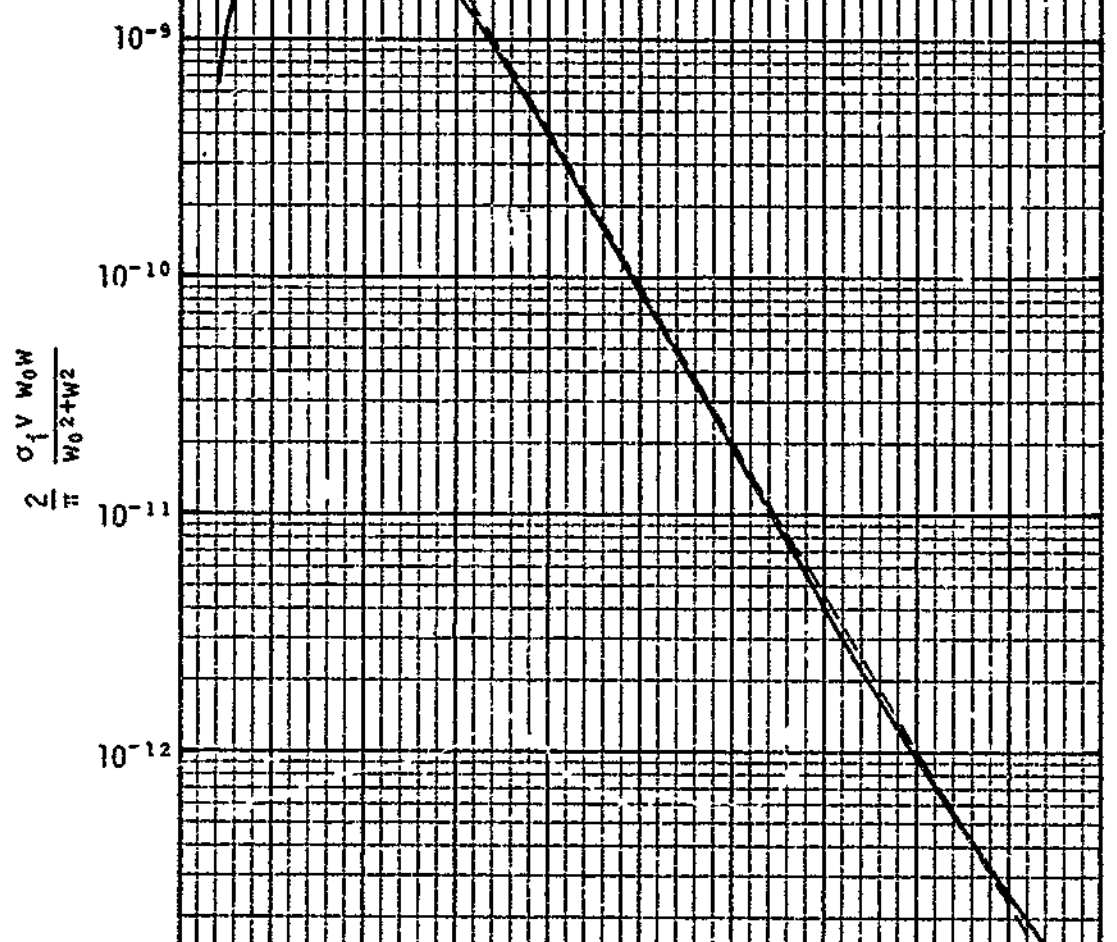

Figure 5. Solid curve, integrand of Eq. (82). Dashed line, fit for higher energies.

These considerations suggest a way of estimating the ionization rate at later times. From Fig. (5) we see that the higher energy part of the differential ionization rate can be fitted quite well by the straight dashed line, which represents the formula

$$dR_0 \simeq N \left[3.2\times10^{-6} e^{-1.3u}\right] du, \tag{85}$$

where

$$u = \ln w \qquad \text{(base e)}. \tag{86}$$

On the other hand, from Eq. (81) we see that the fractional amount of secondary energy per unit u is

$$dF = 0.091\ du. \tag{87}$$

The amount of secondary ionization that will be eventually produced by dF is therefore

$$dI_2 = 1.52\ dF = 0.138du. \tag{88}$$

We estimate the lifetime $T(u)$ for producing this ionization to be

$$T(u) = \frac{dI_2}{dR_0} = \frac{10^5}{2.32N} e^{1.3u} . \tag{89}$$

Thus at time T after production of the secondaries, all of those secondaries will be exhausted which had initial u less than

$$u(T) = \frac{1}{1.3} \ln\left[2.32\times10^{-5}NT\right]. \tag{90}$$

The surviving secondaries (of higher energy) are at this time creating ionization at the rate

$$R(T) \approx N \int_{u(T)}^{u_{max}} (3.2\times10^{-6} e^{-1.3u})\, du, \qquad (91)$$

or, from Eq. (90)

$$\frac{R(T)}{N} \approx \frac{3.2\times10^{-6}}{1.3} \frac{1}{2.32\times10^{-5}} \left[\frac{1}{NT} - \frac{1}{NT_{max}}\right] \qquad (92)$$

$$\approx 0.106 \left[\frac{1}{NT} - \frac{1}{NT_{max}}\right] .$$

Here NT_{max} could be found from Eq. (89) using the maximum u; however, we shall not evaluate T_{max} yet.

First, we shall increase R(T), over the result (92), by 50% on the grounds that some of the tertiary electrons made will also produce ionization, thus assisting the secondaries; thus we raise the factor 0.106 to 0.160. Second, we write R(T) in a form which also agrees with the result (83) at T=0. Thus we write

$$\left.\begin{aligned} R(T) &\approx \frac{\left(1.04\times10^{-6}\frac{cm^3}{sec}\right)N}{1 + \frac{NT}{1.54\times10^{7}}} \quad \text{for } T < T_{max} , \\ &\approx 0 \text{ for } T > T_{max} . \end{aligned}\right\} \qquad (93)$$

T_{max} can now be found by setting

$$1.52 = \int_0^{T_{max}} (R(T)\, dt = 0.160\, \ell n\left(1 + \frac{NT_{max}}{1.54\times10^{7}}\right) ,$$

which yields

$$NT_{max} = 2.0\times10^{11} \text{ sec/cm}^3 . \qquad (94)$$

The amount of secondary ionization $I_2(T)$ produced by time T, per secondary electron, is

$$I_2(T) = 0.160 \ln\left(1 + \frac{NT}{1.54\times10^7}\right) . \quad (95)$$

Thus $I_2(T)$ increases only slowly with time, and reaches half its final value at

$$NT_{1/2} \simeq 10^{-2}\, NT_{max} \simeq 2\times10^9 \text{ sec/cm}^3 . \quad (96)$$

In EMP, one is often interested in the amount of ionization produced in a time of 10^{-8} second after loss of a given amount of energy by the primary (Compton recoil electron). Per 34 ev lost by the primary, the number of ion pairs formed by this time is

$$N_{ip} = \frac{34}{86}\left[1 + 0.160 \ln\left(1 + \frac{N}{1.54\times10^{15}}\right)\right] . \quad (97)$$

This number is given in Table 5 as a function of altitude. One sees that the effect of the time lag in formation of the secondary ionization is an important effect at altitudes above 40 km or so.

Table 5

Altitude, km =	0	10	20	30	40	50
N_{ip} =	1.00	0.98	0.90	0.79	0.69	0.61

9. Electron Equilibration

Once the secondary, tertiary, etc., electrons have fallen below about 15 ev, they can no longer produce additional ionization. However, they still lose energy in collisions with air molecules. If an electric field E is present, the electrons gain energy from it. After some time, the electrons reach an equilibrium distribution in energy, in which energy lost to air molecules is balanced by energy gained from the electric field. This equilibrium distribution depends only on the ratio E/p, where p is the air pressure, if the air temperature is assumed constant.

In EMP calculations, it is usually assumed that the electrons acquire the equilibrium distribution immediately after birth, and also follow changes in E (or E/p) without time lag. Under this assumption, such important quantities as the electron attachment rate (to O_2), the electron drift velocity or mobility, and the cascading rate or Townsend coefficient, depend only on the instantaneous value of E/p. Conveniently, experimental data for these quantities is usually obtained as functions of E/p. Thus, in this approximation, it is not necessary to know the details of the electron energy distribution.

If we now wish to take into account the deviations from equilibrium, including time lags, we shall have to introduce parameters which characterize the electron energy distribution. The simplest such characterization is to use only the mean energy of the distribution. Actually, the parameter U_e of electron swarm theory is 2/3 of the mean energy, in analogy to temperature, although the energy distribution is not Maxwellian if an electric field is present.

We have seen in Sec. 8 that about 70% of the electrons have energy less than 16 ev at birth. Most of the other 30% drop rapidly (in a time given by Eq. (84) below 16 ev by producing further ionization. Therefore, it seems reasonable to start the electrons off, in equilibration calculations, with a mean energy of about 8 ev, or U_e about 5 ev.

Baum (Ref. 7) has studied the relaxation of U_e, using data on momentum and energy transfer collision frequencies provided by A.V.Phelps. We may use Baum's results to appraise the importance of the finite relaxation time for EMP calculations. We take as a typical electric field 1 esu = 3×10^4 volt/meter. Table 6 then shows, for various altitudes, the equilibrium value of U_e and the time to reach equilibrium, starting from U_e = 5 ev. One sees that, for the electric field assumed, the times are all less than 10^{-9} second. It therefore appears that the finite relaxation time cannot have a drastic effect (by altering the effective

electron mobility) on the peak electric field, unless the computed electric field changes appreciably in 10^{-9} seconds.

Table 6

altitude, km =	0	10	20	30	40
U_e, ev =	0.17	0.35	1.0	1.6	∿5
time, sec =	7×10^{-10}	9×10^{-10}	3×10^{-10}	3×10^{-10}	$\sim10^{-10}$

Note that at 40 km, the equilibrium U_e is high enough that, for a Maxwell distribution of electron energies, cascading would occur rapidly. However, for high U_e, the deviations from the Maxwellian distribution are large. To compute the cascading rate correctly, one would need more information (than U_e) concerning the electron distribution. However, there does not appear to be enough basic cross-section data available (currently) to permit an adequate treatment of the detailed distribution. Thus the cascading rate can be computed only for the equilibrium case, where it is known from the Townsend coefficient, which has been determined experimentally as a function of E/p. The determination of the cascading rate from the data on the Townsend coefficient is discussed in Ref. 8.

At low altitude, where cascading normally is not important, one could devise a non-equilibrium correction by using Baum's relaxation times. It would be important to do this only if rise times of the electric field are as short as 10^{-9} second.

References

(1) See the review article by Bethe and Ashkin in "Experimental Nuclear Physics", E. Segre, editor, Vol.I, Wiley, 1953; p.253

(2) See the discussion in Mott and Massey, "The Theory of Atomic Collisions", Third Edition, Oxford, 1965; p.467

(3) See Longmire, "Elementary Plasma Physics", Wiley-Interscience, 1963; p.199

(4) Marshall and Ward, Can. J. Research, A15, 39 (1937)

(5) H.A. Bethe, Ann Physik, 5, 325 (1930); also Z. Physik, 76, 293 (1938)

(6) B.L. Schram, F.J. DeHeer, M.J. Van der Wiel and J.Kistemacher, Physica, 31, 94 (1965)

(7) AFWL EMP 2-1, Electromagnetic Pulse Theoretical Notes, Volume I, Note 12, by C.E.Baum.

(8) MRC-R- 3 , "Development of the CHAP EMP Code (U)", by H.J. Longley and C.L.Longmire, in publication, Unclassified